THE JOURNAL OF PHYSICAL CHEMISTRY B

Article

pubs.acs.org/JPCB

Solid-State Spectroscopic Characterization of α-Chitins Deacetylated in Homogeneous Solutions

Kai Zhang,*[†,⊥] Andreas Geissler,[†] Steffen Fischer,[†] Erica Brendler,[‡] and Ernst Bäucker[§]

[†]Institute of Plant and Wood Chemistry, Dresden University of Technology, Pienner Strasse 19, D-01737 Tharandt, Germany

[‡]Institute of Analytical Chemistry, Freiberg University of Mining and Technology, Leipziger Strasse 29, D-09599 Freiberg, Germany

[§]Institute of Forest Utilization and Forest Technology, Dresden University of Technology, Pienner Strasse 19, D-01737 Tharandt, Germany

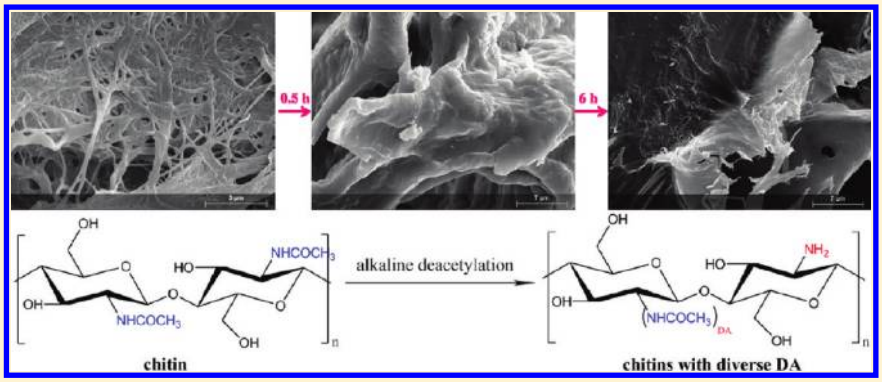

ABSTRACT: Synthesis and spectroscopic characterization of α-chitins exhibiting degrees of acetylation (DA) between 0.5 and 1 were reported. Crab shell α-chitin consisting of microfibrils with a width of less than 1 μm was regenerated from or alkaline deacetylated in 30% aqueous NaOH solution. After the deacetylation in homogeneous solution, the DA of α-chitins decreased steadily with prolonged deacetylation times from 1 to 0.54. The native microfibrils of starting α-chitin were destroyed, while aggregates or sheets were formed depending on the DA of chitins. According to WAXD measurements, deacetylated chitins with DA lower than 0.76 have different crystalline structures than starting α-chitin. Furthermore, FT Raman spectroscopy demonstrated a novel rapid method to determine the DA of chitin with correlation coefficients greater than 0.99. On the basis of the FT Raman signals ascribed to the amide groups, the amount of hydrogen bonds linked to C═O groups decreased strongly with lower DA and the relationship between them was presented.

INTRODUCTION

Chitin is a naturally occurring polysaccharide and consists of linearly β-(1−4)-linked *N*-acetylglucosamines.[1] At least three natural anhydrous crystalline allomorphs of chitin, α, β and γ-chitin, have been found and the α-chitin is the most stable thermodynamically. The β and γ-chitin can be irreversibly converted into α-chitin, for example, after an alkaline treatment.[2]

It is generally accepted that chitin has a degree of acetylation (DA) of more than 50%, while chitosan exhibits a DA lower than 50%.[1] The adjustment of DA can be achieved after heterogeneous alkaline deacetylation of chitin, for example, using 40−50% aqueous NaOH solution at elevated temperatures.[3,4] After the deacetylation, chitins with various DA could be obtained. The DA is a very important feature affecting the properties of chitins, for example, the solubility, aggregation and physicochemical properties.[5−7] Various methods have been developed for the determination of the DA of chitin and chitosan, for example, spectroscopic and titration methods.[8−12] Among them, the spectroscopic methods involving IR and NMR spectroscopy are well established in last decades.[8,9,13,14] Using IR spectroscopy, diverse absorption band ratios can be used for the determination of DA.[8,9] ^{1}H NMR spectroscopy provides accurate results and ^{13}C NMR spectroscopy can be used to determine DA over the entire range.[9,13,14] Despite their wide use, they still have disadvantages including the influence of highly polar system (IR), dependence on the choice of baseline (IR), requirement of sample preparation (IR, ^{1}H NMR), long time for measurement (^{13}C NMR) and availability of the instrument (NMR). In contrast, Raman spectroscopy as a rapid and nondestructive analysis method does not have these problems.[15,16] Furthermore, it has demonstrated the feasibility of determining the degrees of substitution of chitosan derivatives.[17]

Apart from DA, the crystallinity and the morphology of chitins from distinct sources differ from each other.[18] The crystalline structure of chitin and chitosan could be analyzed via X-ray diffraction as well as IR spectroscopy.[19−21] After an

Received: October 31, 2011
Revised: March 22, 2012
Published: March 27, 2012

Scheme 1. Schematic Representation of Alkaline Deacetylation of Chitin

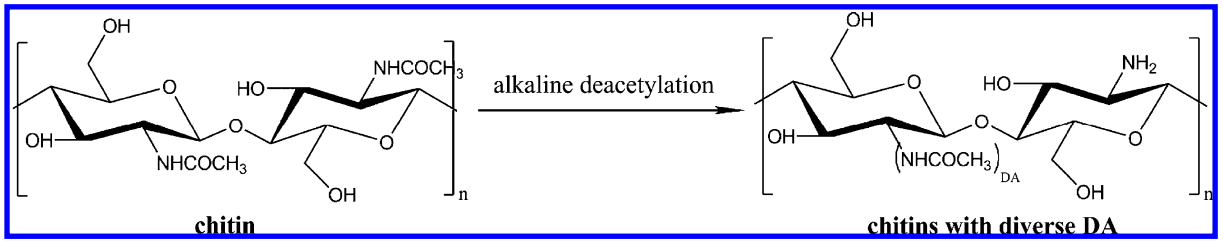

alkaline treatment or the regeneration of chitin from its solution, the crystallinity of chitin decreased significantly and the original microfibrils of chitin could be converted into big coagulated fibres.[21−23] Moreover, it was claimed that the DA of chitin could affect its crystallinity and water-solubility. Water-soluble chitins with a DA of ∼49% were proposed to show a different crystal structure than native α-chitin.[5] In a similar way, a semi-α-structure was suggested for regenerated α- and β-chitin from their solutions in BminAc (1-butyl-3-methylimidazolium acetate).[21] However, it is still not clear how the crystal structure of α-chitin changes with its DA.

On the other side, the hydrogen bonds between the functional groups within chitin are important for the formation of crystalline regions. The C═O groups of acetyl groups are suggested to be linked to NH or C(6)OH groups forming hydrogen bonds.[20] The hydrogen bonded network can possibly reflect the crystal structure of chitin, but it can be affected by commonly used heterogeneous deacetylation. This heterogeneous deacetylation can result in noneven distributions of acetyl groups along chitin chains, whereas a uniform distribution of acetyl groups can be achieved under homogeneous deacetylation.[1,3,18]

Thus, in this report, crab shell α-chitin, demonstrating microfibrils with a width of less than 1 μm, was initially dissolved in 30% aqueous NaOH solution. Then, chitins with reduced DA were obtained after the homogeneous deacetylation of starting chitin. These chitins in solid-state were characterized via solid-state CP/MAS ^{13}C NMR, FT Raman spectroscopy, wide-angle X-ray diffraction (WAXD) and scanning electron microscopy (SEM), with the aim to determine their DA, to analyze their crystal structures and morphologies. FT Raman spectroscopy exhibited the feasibility of establishing novel quantifying method for the DA of chitins and also a possibility to analyze hydrogen bonds linked to C═O groups.

EXPERIMENTAL SECTION

Materials. Chitin from crab shell with a molecular weight of 4×10^5 Da was purchased from Carl Roth GmbH (Karlsruhe, Germany). Chitosan with a DA of 5.5% and a viscosity of 147 mPas (1% in 1% acetic acid at 20 °C) were obtained from Heppe medical GmbH (Halle/Saale, Germany). Demineralized water was used in all experiments and other chemicals in analytical grade were used as received.

Ball-Milling of Chitin. Chitin (0.5 g) in 7 mL of water was milled on a ball mill (type = MM 2000) from Retsch (Hahn, Germany) for 30 min (wet-milled chitin). Similarly, a comparable dry-milling of chitin (0.5 g) for 30 min was carried out (dry-milled chitin). After the ball-milling, wet-milled chitin was lyophilized and both ball-milled chitins were stored under vacuum for the SEM measurement.

Dissolution of Chitin. Wet-milled chitin (3 g) was suspended in 200 mL 30% aqueous NaOH solution under stirring. Thereafter, the mixture was frozen and then melted at room temperature (RT). This step was repeated a few times, until an optically transparent solution was obtained, indicating that chitin was dissolved in the 30% aqueous NaOH solution. Then, the solution was centrifuged to separate very minor part of nondissolved particles. Chitin could be regenerated from its alkaline solution by precipitating 25 mL of the chitin solution in 5 volumes ethanol and adjusting the pH value to 7.5 using acetic acid. After that, chitin was separated by centrifugation, washed with water until salt-free and lyophilized until constant weight.

Alkaline Deacetylation of Chitin (Scheme 1). For the deacetylation of chitin, the flask with chitin solution was purged with N_2 gas thoroughly and the solution was kept at 60 °C for 5, 30, 60, 120, 180, 300, and 360 min, leading to DC1, DC2, DC3, DC4, DC5, DC6 and DC7. After the reaction, deacetylated chitins were obtained by precipitating reaction mixture in 5 volumes ethanol and the pH was adjusted to 7.5 with acetic acid. The product was separated by centrifugation, washed with water until salt-free and lyophilized.

Measurements. Solid-state CP/MAS ^{13}C NMR spectroscopy was carried out using a Bruker Avance 400 WB spectrometer (Bruker, Etlingen, Germany) with a frequency of 100.65 MHz, 35 ms acquisition time, 1 ms contact time, a sweep width of 29 400 Hz and a relaxation delay of 3 s at RT. Scans between 5000 and 7000 were accumulated. 7.5-mm rotor with around 0.2 g samples was used for analysis. Chemical shifts in ^{13}C NMR spectra were quoted using tetramethyl silane (TMS) and were obtained according to its chemical shift as 0 ppm. The integrals between 110 and 48 ppm (I_{GlcN}) (GlcN stands for glucosamine units of chitin) as well as between 30 and 19.5 ppm (I_{Ac}) were acquired from the obtained spectra. The DA was calculated according to: $DA = 6 \times I_{Ac}/I_{GlcN}$.

Wide-angle X-ray diffraction (WAXD) was carried out on a XRD 3003T/T X-ray diffractometer (GE Inspection Technologies, U.S.A.) with Cu Kα radiation from 6 to 36° using θ−θ total reflection technique.

Scanning electron microscopy (SEM) images were obtained on a JEOL JSM-T330A scanning microscope (Jeol Ltd., Tokyo, Japan) at RT. Samples were coated with a 30 nm thick carbon and gold layer.

FT Raman spectra of the samples in small aluminum discs were recorded on a Bruker MultiRam spectrometer (Bruker) with a Ge diode as detector that is cooled with liquid-nitrogen. A cw-Nd:YAG-laser with an exciting line of 1064 nm was applied as light source for the excitation of Raman scattering. The spectra were recorded over 3500−150 cm^{-1} using an operating spectral resolution of 3 cm^{-1} and a laser power output of 100 mW. A double analysis per 400 scans was carried out for each sample. An average Raman spectrum was formed

dx.doi.org/10.1021/jp210469x | J. Phys. Chem. B 2012, 116, 4584−4592

afterward and the spectrum was max-min-normalized on the peak at 1380 cm^{-1} using the operating spectroscopy software OPUS Ver. 6.5 (Bruker).

RESULTS AND DISCUSSION

Ball-Milling and Dissolution of Crab Shell α-Chitin. Before being dissolved in 30% aqueous NaOH solution, starting α-chitin was ball-milled in the presence or absence of water, resulting in wet- and dry-milled chitins, respectively. After the ball-milling, the wet- and dry-milled chitins were subjected to preparing the solution of chitin in 30% aqueous NaOH solution. The wet-milled chitin could be almost completely dissolved in 30% aqueous NaOH solution, while dry-milled chitin was not totally dissolved.

According to the WAXD diffractogram of dry-milled chitin (Figure 1), characteristic crystalline reflections for α-chitin, indexed as 020, 021, 110, 120, 101, and 013, strongly decreased or even disappeared. In comparison, these reflections are still visible within the WAXD diffractogram of wet-milled chitin. Therefore, chitin became less crystalline after dry-milling than wet-milling. However, dry-milled chitin could not be quantitatively dissolved in 30% aqueous NaOH solution. According to the SEM images in Figure 2, wet- and dry-milled chitin demonstrated different morphologies after the ball-milling. It is visible that wet-milled chitin contains the microfibrils of native α-chitin after the ball-milling under neutral conditions. These microfibrils have a width of less than 1 μm and a length of a few μm (Figure 2, a1 and 2). Water was probably very important for the maintenance of the original morphology of chitin microfibrils during the ball-milling, because chitin was big crystals after the dry-milling (Figure 2, b1 and 2). The formation of big chitin crystals possibly hampered the dissolution of chitin in aqueous NaOH solution due to reduced contact areas. It was assumed that the high crystallinity of chitin is an essential factor influencing its solubility.[5,22] As shown in this study, the surface morphology of chitin, especially the contact area between chitin and its solvents, strongly affect the solubility of chitin.

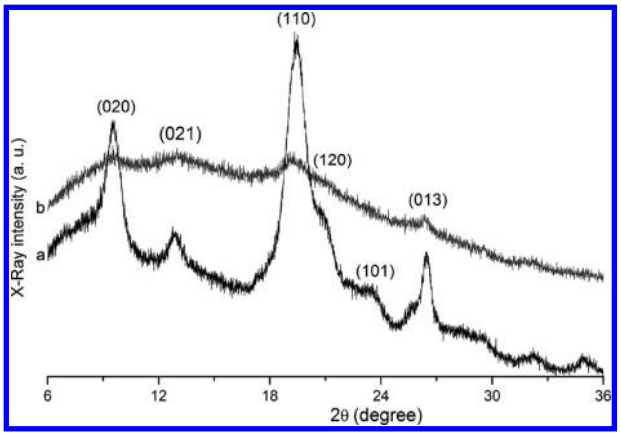

Figure 1. WAXD diffractograms (6−36°) of lyophilized (a) wet-milled chitin and (b) dry-milled chitin at RT.

Deacetylation of Starting α-Chitin. After the deacetylation of starting α-chitin in 30% aqueous NaOH solution at 60 °C for up to 360 min, various deacetylated α-chitins were prepared. A regenerated α-chitin was obtained by precipitating the solution of starting α-chitin in ethanol without further deacetylation. The degree of acetylation (DA) of starting chitin, regenerated chitin and deacetylated chitins were determined via solid-state CP/MAS ^{13}C NMR spectroscopy.[13] Regenerated chitin without further deacetylation has a DA of approximate 1, indicating that the dissolving process at low temperature (max. RT) did not cause a deacetylation of chitin. However, the deacetylation at 60 °C after 5 min led to a significant decrease of DA to 0.92, indicating that the high temperature promotes the homogeneous deacetylation of chitin. After the homogeneous deacetylation of up to 360 min, DA were determined to be between 0.92 and 0.54 (Figure 3).

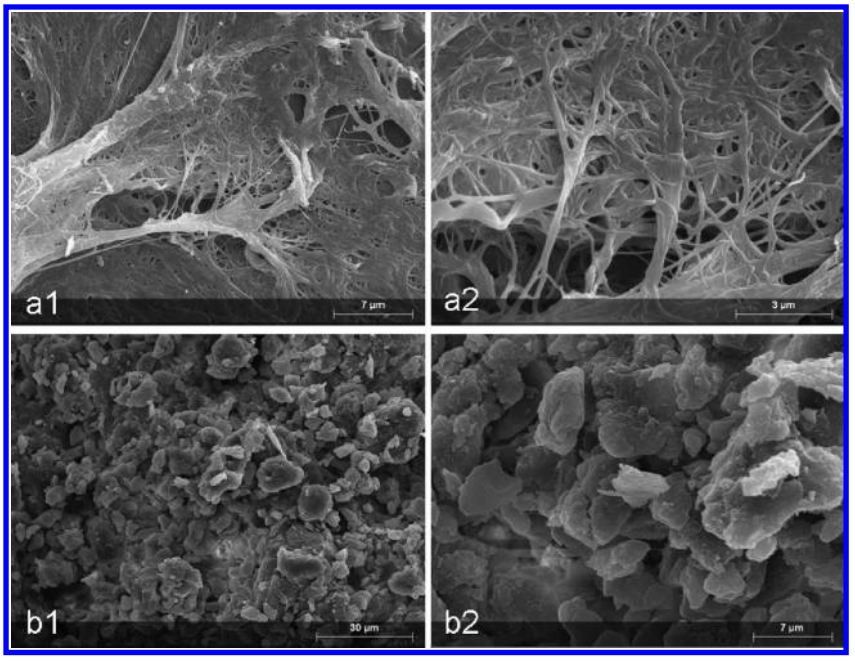

Figure 2. SEM images in two distinct magnifications of lyophilized (a) wet-milled chitin (the scale bar is 7 and 3 μm in a1 and a2) and (b) dry-milled chitin (the scale bar is 30 and 7 μm in b1 and b2).

dx.doi.org/10.1021/jp210469x | J. Phys. Chem. B 2012, 116, 4584−4592

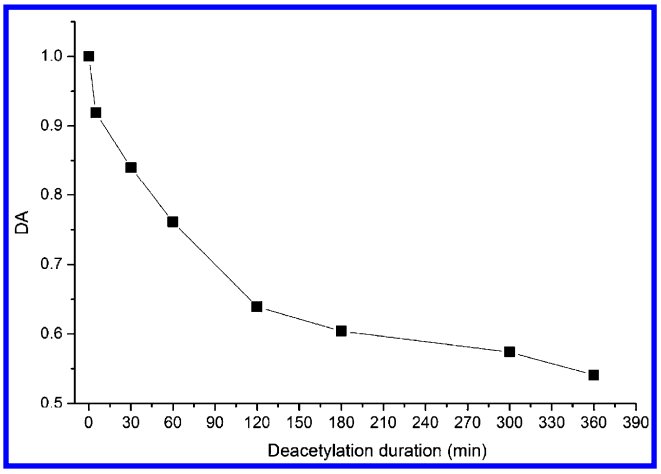

Figure 3. Development of DA of deacetylated chitins together with deacetylation duration in min. Regenerated chitin is referred as deacetylated chitin after 0 min deacetylation.

As reported before, elevated temperature is also needed for the deacetylation under heterogeneous conditions. High concentration of NaOH solution, for example, 50% and high temperature, for example, 80−110 °C, were used for the deacetylation of chitin.[3,4,7,24,25] After 120 min one-step heterogeneous deacetylation, resulted water-insoluble deacetylated chitin showed a DA of only 36.2%.[24] In constrast, deacetylated chitin with a DA of 0.64 was obtained after 120 min homogeneous deacetylation in present report. This difference may primarily be due to the different concentrations of NaOH solution and deacetylation temperature. The concentration of NaOH solution and the deacetylation temperature for the homogeneous deacetylation are both lower than those reported for the heterogeneous one.[24,25] Consequently, the homogeneous deacetylation is slower and deacetylated α-chitins with DA higher than 0.5 were obtained even after 360 min deacetylation (Figure 3).

Moreover, the deacetylation proceeded preliminarily within the first 120 min and became very slow afterward. A similar effect has also been found for the heterogeneous deacetylation of chitin.[26,27] It was shown that α-chitin was strongly deacetylated during the first 30 min, which was proposed to be a pseudofirst-order reaction.[24] Based on the fact that the DA decreased fast in the first 120 min and then leveled off, the deacetylation of chitin in homogeneous solution is also a pseudo-first-order reaction. However, this homogeneous deacetylation needed longer time than the heterogeneous one to reach a comparable DA.

Characteristic solid-state CP/MAS ^{13}C NMR spectra of starting chitin and deacetylated chitins represent well resolved peaks (Figure 4), which are typical for α-chitin.[28] The peaks at 173.8 and 23 ppm are ascribed to the carbons within carbonyl and methyl groups, respectively. Other signals attributed to the carbons in the repeating units of chitin are visible in the range of 48−110 ppm and can be assigned to the carbons in GlcN units (Table 1).[13,28]

Because no chemical modification of the primary hydroxyl groups took place, the intensity and position of the C6-signal should stay stable within the solid-state CP/MAS ^{13}C NMR spectra of deacetylated chitins. By normalizing these NMR spectra using the peak intensity of the C6-signal (Figure 4), it is visible that the intensities of other signals besides the signal of C5 decrease significantly with falling DA. The stability of the intensity of C5's peak indicates the correlation of the spins of C5 with those of C6. The decrease of the intensities of other signals with lower DA reveals the structural correlations between C2 and C1/3/4 in chitin.

According to Figure 4 and Table 1, significant differences are notable in the range of 50 and 80 ppm within the solid-state CP/MAS ^{13}C NMR spectra. The signal of C3 at 73.5 ppm is visible within the solid-state CP/MAS ^{13}C NMR spectra of chitins with high DA, e.g. starting chitin and DC1. After 60 min deacetylation, it becomes very weak within the solid-state CP/MAS ^{13}C NMR spectrum of DC3 (DA = 0.76). However, this signal is not notable within the solid-state CP/MAS ^{13}C NMR spectrum of deacetylated chitins with a lower DA, for example, DC4 exhibiting a DA of 0.64 (Figure 4). On the other side, a broad signal emerges at 75.5 ppm which is ascribed to C3 and C5. The presence of this combined signal has also been observed for the amorphous β-chitin.[28,29] Because the alkaline treatment of β-chitin results in the conversion into α-chitin,[2,23] it is very possible that a different structure from α- and β-chitin was formed for the deacetylated α-chitins with a DA of less than 0.76.

Furthermore, the intensity of the signal at 55.3 ppm decreases strongly with falling DA. Within the solid-state CP/MAS ^{13}C spectrum of DC7 with a DA of 0.54, it demonstrates only a shoulder. However, a new signal occurs at 58 ppm and

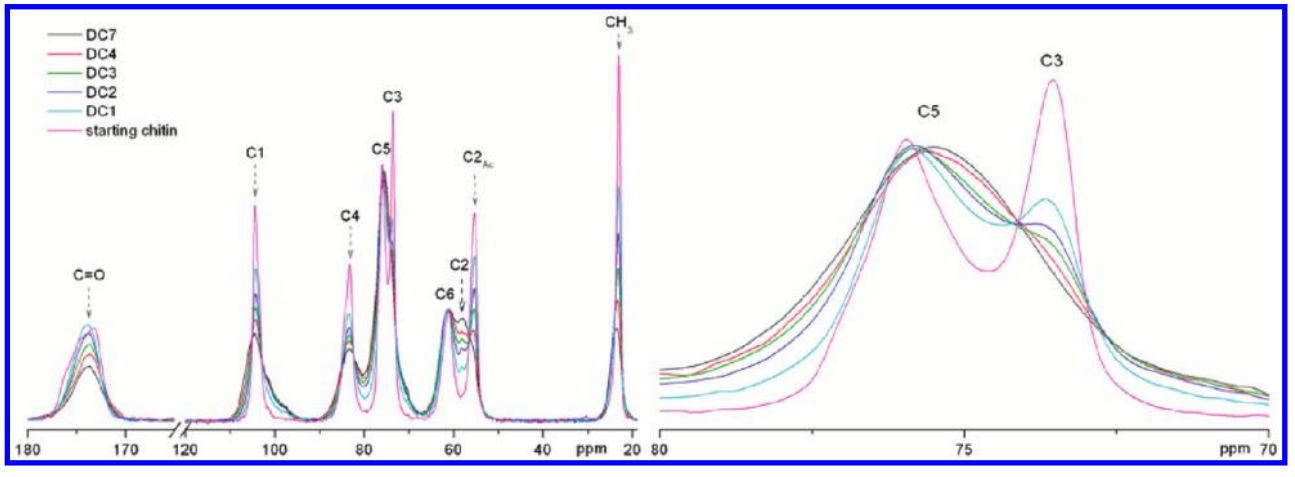

Figure 4. Solid-state CP/MAS ^{13}C NMR spectra (left, 180−19.5 ppm; right, 80−70 ppm) of starting α-chitin, DC1, 2, 3, 4, and 7 at RT.

dx.doi.org/10.1021/jp210469x | J. Phys. Chem. B 2012, 116, 4584−4592

Table 1. Assignment of the Signals within the Solid-State CP/MAS ^{13}C NMR Spectra of Starting and Deacetylated Chitins in Figure 4[a]

samples	C═O	C1/C1́	C4	C5	C3	C6	C2	$C2_{Ac}$	CH3
chitin	173.8	104.4	83.2	75.5	73.5	61.2		55.3	23
DC7	173.7	104.5	83.4	75.5	75.5	61	58	shoulder	23.5

[a]The values are chemical shifts in parts per million.

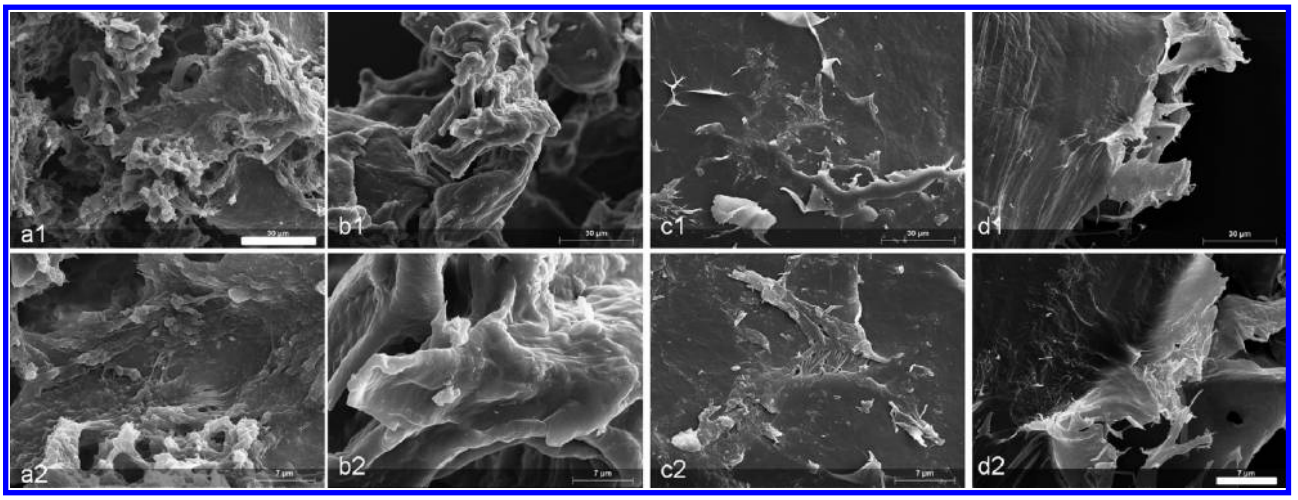

Figure 5. SEM images in two distinct magnifications of (a) regenerated chitin (DA = 1), (b) DC2 (DA = 0.84), (c) DC3 (DA = 0.76), and (d) DC7 (DA = 0.54) (the scale bar is 30 and 7 μm in upper and lower line, respectively).

its intensity increases with falling DA. Within the solid-state CP/MAS ^{13}C spectrum of starting α-chitin, only the signal at 55.3 ppm is visible and no signal at 58 ppm is present. Thus, the peak at 55.3 ppm is ascribed to C2 with the acetylation at 2-N-position, while the signal at 58 ppm is attributed to C2 without acetylation.

In addition, the signals of C1 and C4 within the solid-state CP/MAS ^{13}C NMR spectra of chitins with lower DA are slightly broader than those of chitins with higher DA, suggesting a slightly less crystalline structure.[28]

Morphology. Figure 5 contains SEM images of regenerated chitin and deacetylated chitins. After the regeneration, only small aggregates instead of microfibrils of chitin are notable (Figure 5a). After 30 min deacetylation, the aggregates of chitin exhibiting smooth surface grew. However, with prolonged deacetylation duration through 60 to 360 min, DC3 and DC7 demonstrate large sheets with smooth surfaces.

The crab shell is suggested to be consist of chitin-protein networks in a twisted plywood structure (Bouligand structure). The Bouligand layers could be 3−5 μm in exocuticle and 10−15 μm in endocuticle. These layers are composed of chitin/proteins fiber with a diameter of up to 300 nm.[30] However, the chitin nanofibers were changed into coagulated masses after a treatment with 30% aqueous NaOH solution or 8 N HCl, as described for β-chitin.[23] In this report, these modified chitins exhibit uniform but different morphologies. This fact may be due to their distinct DA, because other processes including the regeneration and drying proceeded under equal conditions. During the dissolution of starting chitin, the original chitin microfibrils were destructed and the hydrogen bonds network of starting chitin was broken. During the subsequent regeneration, the chitin chains bound with each other and small aggregates were formed. With more hydrophilic amino groups in the chitin chains, larger aggregates were generated (Figure 5b), which is possibly due to the formation of a new hydrogen bonded network between these chitin chains. In particular, the amino groups may contribute substantially to the formation of these hydrogen bonds by interacting with O6.[31,32]

However, with more amino groups in the chains, uniformly structured sheets instead of aggregates could be obtained. This is possibly due to the formation of a different hydrogen bonded network. As reported before, the NH-groups form hydrogen bonds with O6 within the crystals of chitosan, while the NH-groups interact with C═O groups within the crystals of chitin.[20,31−33]

Figure 6 displays characteristic WAXD diffractograms of starting, regenerated chitin and deacetylated chitins. Regenerated chitin or DC2 (DA = 0.84) after an alkaline deacetylation of 30 min presented very similar diffractograms to that of starting α-chitin, indicating the reformation of the original crystalline structure. At the same time, the signals at

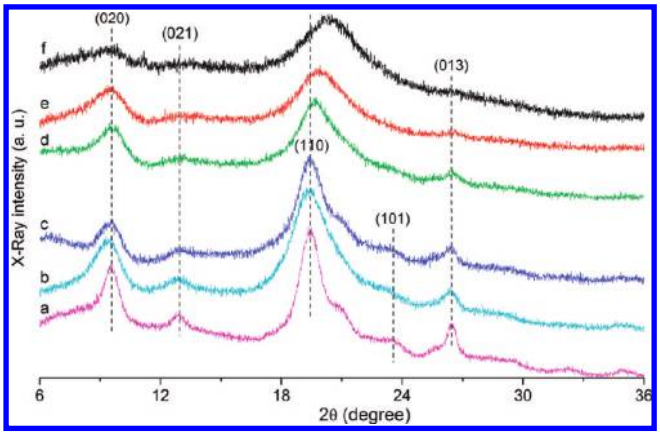

Figure 6. WAXD diffractograms (6−36°) of (a) starting chitin, (b) regenerated chitin, (c) DC2 (DA = 0.84), (d) DC3 (DA = 0.76), (e) DC4 (DA = 0.64), and (f) DC7 (DA = 0.54) at RT.

dx.doi.org/10.1021/jp210469x | J. Phys. Chem. B 2012, 116, 4584−4592

19.4° and 26.5° within the WAXD diffractograms of deacetylated chitins become broader and weaker, showing the presence of more amorphous material.

After the deacetylation for up to 360 min, typical signals for α-chitin at 9.5°, 23.5°, and 26.5° attributable to 020, 101, and 013 plane stay at the constant positions with lower intensities.[20−22] This fact demonstrates a continuous reduction of the content of α-crystalline structure along with lower DA (Figure 6). After 60 min deacetylation, DC3 with a DA of 0.76 showed a slight shift of the signal attributed to the 110 plane from 19.4° to 19.7°.[20,21] After longer deacetylation durations of 120 (DC4) and 360 min (DC7), this signal shifted through 19.9° to 20.4°. The shift of this signal has also been found for regenerated α-chitin from its BminAc solution.[21] Thus, deacetylated chitins with DA of less than 0.76 exhibit possibly a different crystalline structure than α-crystalline structure. Probably, only the chitins with high DA of more than 0.76 could form a similar crystalline structure to α-chitin.

Furthermore, it was reported that the heterogeneously alkaline treatment of chitin led to a decrease of the crystallinity of chitin. This decrease was dependent on the duration of the alkaline treatment.[22] Moreover, if α-chitin was regenerated from its solution, a modification of the α-crystalline structure was detected and the formation of a semi-α-structure was proposed.[5,21] In this report, the deacetylation of starting chitin in its NaOH solution proceeded under equal conditions for different deacetylation times. The drying processes of deacetylated chitins from the solution were nearly identical. Therefore, the DA, that is, the content of acetyl groups, may primarily affect the crystalline structure of these chitins. A higher content of acetyl groups can form hydrogen bonds with NH-groups, leading to the formation of α-crystalline structure. In contrast, the deacetylated chitins with lower DA contain fewer acetyl groups but more amino groups. Following that, a different hydrogen bonded network may be generated with a different crystalline structure (Figure 4 and 6).[21,31,32] Thus, the alkaline deacetylation of α-chitin can modify the crystalline structure for deacetylation times longer than 60 min.

Moreover, it was assumed that the distribution of acetyl groups along the chitin chains also affects the solubility of chitin in addition to DA and molecular weight.[34−36] After a homogeneous deacetylation, the acetyl groups should be randomly distributed along chitin chains, while the heterogeneous deacetylation led to blockwise distribution of acetyl groups.[3] Chitin with randomly distributed acetyl groups is supposed to have greater water-solubility for the same DA. In the present report, the obtained deacetylated α-chitins were not water-soluble after homogeneous deacetylation. High DA (more than 0.5) and the presence of crystalline regions in these chitins as shown above are probably the major reasons for their insolubility in water. The DA is possibly the most important factor affecting the water-solubility of chitin, as proposed before.[35]

FT Raman Spectroscopic Analysis. Figure 7 displays characteristic FT Raman spectra of starting, regenerated α-chitin and chitosan. Starting and regenerated α-chitin demonstrate almost identical Raman spectra, while chitosan has a quite different Raman spectrum.

The characteristic signals were listed in Table 2 and assigned. According to the FT Raman spectra in Figure 7, following significant differences are visible.

First, starting and regenerated chitin display three peaks at 2964, 2937, and 2882 cm^{-1}, while chitosan shows a peak at 2885 cm^{-1} with a shoulder at 2928 cm^{-1}. The band at 2964 cm^{-1} was attributed to asymmetric stretching vibrations of CH_3 groups.[37] The peak at 2937 cm^{-1} and the shoulder at 2928 cm^{-1} are derived from stretching vibrations of C−H groups within the acetyl groups at. The signals at 2882 and 2885 cm^{-1} are ascribed to stretching vibrations of C−H groups in GlcN units.[17,38]

Second, the signals at 1660 and 1621 cm^{-1} are notable within the FT Raman spectra of starting and regenerated chitin, while chitosan demonstrates only a band at 1591 cm^{-1}. The signals at 1660 and 1621 cm^{-1} are ascribed to amide I vibrations of the amide groups within chitin.[29,37] The two signals ascribed to amide I vibrations are attributed to the presence of two different types of hydrogen bonds in α-chitin crystals.[20,37] The band at 1591 cm^{-1} is ascribed to deformation vibrations of NH_2-groups.[29,38]

Third, the bands at 1329 and 956 cm^{-1} are only visible within the FT Raman spectra of starting and regenerated chitin, but not observable within the FT Raman spectrum of chitosan. These bands are ascribed to amide III vibrations (C−N stretching vibrations) (1329 cm^{-1}) and C−CH_3 deformation vibrations (956 cm^{-1}), respectively.[38,39]

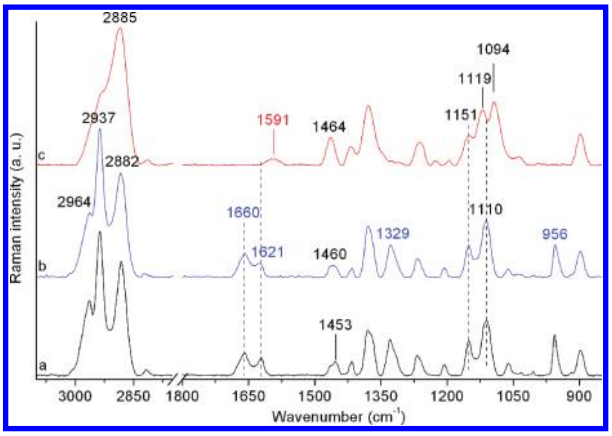

Figure 7. FT Raman spectra (3100−850 cm^{-1}) of (a) starting α-chitin, (b) regenerated chitin, and (c) chitosan at RT.

Table 2. Assignment of FT Raman signals between 3100 and 800 cm^{-1} (Figure 7)

bands in cm^{-1} (chitin)	bands in cm^{-1} (chitosan)	vibrational modes
2964		$\upsilon_{as}(CH_3)$
2937	2928	υ(C−H of CH_3)
2882	2885	υ(C−H of ring)
1660		amide I band (C═O)
1621		amide I band (C═O)
	1591	$\delta(NH_2)$
1453	1464	$\delta(CH_2)$
1416	1416	$\delta(CH_2)$, δ(HCC), δ(HCO), δ(COH)
1380	1380	$\delta(CH_2)$, δ(HCC), δ(HCO), δ(COH)
1329		amide III
1151	1151	υ_{asym}(COC), glycosidic
1110	1119	υ_{sym}(COC), glycosidic
	1094	υ_{sym}(COC), glycosidic
956		δ(C−CH_3)
898	898	CH_x deformation

dx.doi.org/10.1021/jp210469x | J. Phys. Chem. B 2012, 116, 4584−4592

Moreover, a new band at 1094 cm^{-1} emerges within the FT Raman spectrum of chitosan, which is due to the symmetric stretching vibrations of glycosidic COC-groups.[40] However, this band is not visible within the FT Raman spectrum of starting or regenerated α-chitin. Possibly, this vibration is hampered due to the highly crystalline structure of chitins.[18,29]

Finally, shifts of the peak maxima of the bands around 1460 and 1110 cm^{-1} are visible. The shift of the peak maximum from 1453 through 1460 to 1464 cm^{-1} is due to conformational changes of polysaccharides, while the shift of the band from 1110 to 1119 cm^{-1} is ascribed to the elimination of acetyl groups and the presence of NH_2-groups.[40]

Figure 8 depicts normalized FT Raman spectra (1800−800 cm^{-1}) of starting chitin and deacetylated chitins. The band at

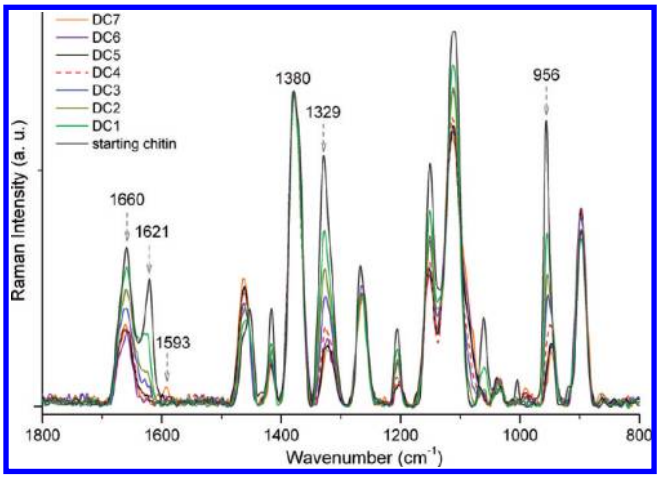

Figure 8. FT Raman spectra (1800−800 cm^{-1}) of starting chitin and deacetylated chitins (DC1−7) at RT. The Raman spectra were normalized on the band at 1380 cm^{-1}.

1380 cm^{-1} is ascribed to various deformation vibrations of polysaccharides' backbones, for example, δ(CH2), δ(HCC), δ(HCO), and δ(COH).[17,40] Its intensity should be independent of the DA of chitin. Thus, this band can be used as internal standard for the normalization of the FT Raman spectra of chitins.[17] The Raman bands in the range between 1800 and 800 cm^{-1} are listed in Table 2. As shown in Figure 8, the intensities of the signals at 1660, 1621, 1416, 1329, 1151, 1110, and 956 cm^{-1} decrease significantly with lower DA.

The band at 1660 cm^{-1} is notable within the FT Raman spectra of all chitins, while the band at 1621 cm^{-1} is only visible within the FT Raman spectra of the deacetylated chitins with DA of more than 0.64 (DC4). The bands at 1660 and 1621 cm^{-1} represent the vibrations of C═O groups which are involved in the formation of hydrogen bonds with NH and/or C(6)OH groups,[20,37] although the types of hydrogen bonds (intermolecular or intramolecular) are still not clear.[33] However, the disappearance of the band at 1621 cm^{-1} reflects changes of the hydrogen bonded network or the crystal sizes.

Within the FT Raman spectrum of DC7 with a DA of only 0.54, a new band at 1593 cm^{-1} emerges. This band is ascribed to the N−H deformation vibrations.[29,38] However, it is not observable within the FT Raman spectra of chitins with higher DA. High amounts of NH_2-groups within the chains of chitin/chitosan are possibly necessary because of their weak inherent Raman intensity.

Using the area under the band at 1329 or 965 cm^{-1} as a Raman analysis parameter, predicted DA were obtained for the real DA of each chitin. The relationships between predicted DA and real DA of chitins were demonstrated by linear calibration curves with correlation coefficients (r) greater than 0.99 (Figure 9). Thus, FT Raman spectroscopy provides a novel

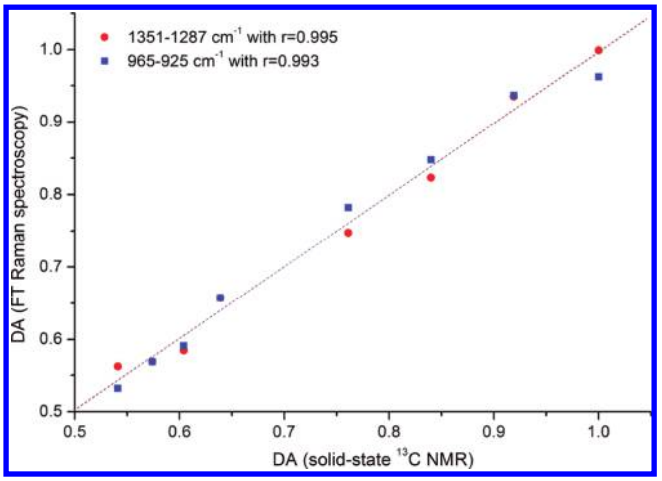

Figure 9. Calibration curves obtained after plotting the DA of chitins obtained using FT Raman spectroscopy against the DA determined by solid-state ^{13}C NMR. The areas of two diverse bands (as in the Figure) were used as Raman analysis parameters yielding two calibration curves.

rapid and nondestructive quantifying method for the determination of the DA between 0.5 and 1. Moreover, the excellent correlations between the DA predicted by FT Raman spectroscopy and the DA measured by solid-state ^{13}C NMR of these chitins confirm that FT Raman spectroscopy can be used to quantitatively characterize chitins.

As described before, the C═O groups of acetyl groups are involved in the hydrogen bonds with NH and/or C(6)OH groups.[20,29,37] The Raman bands at 1660 and 1621 cm^{-1} represent the C═O groups involved in hydrogen bonds. Thus, based on these Raman bands (Figure 10), the relative amounts of C═O groups in modified chitins in comparison to starting chitin, and therefore the relative amounts of hydrogen bonds linked to C═O groups, can be calculated. For this purpose, the areas under the Raman bands in the range of 1688−1604 cm^{-1} were determined and the percentages compared to starting chitin were calculated (Figure 10). It is clear in Figure 10 that the regeneration of chitin from its solution resulted in a significant reduction of hydrogen bonds linked to C═O groups from 100% to ca. 87%, although the DA of regenerated chitin is still 1. Furthermore, after the deacetylation of at least 120 min (DC4 with a DA of 0.64), the contents of hydrogen bonds linked to C═O groups were less than 35% of starting chitin. In fact, the band at 1621 cm^{-1} is not observable within the FT Raman spectra of deacetylated chitins with a DA of maximal 0.64 (Figure 10). The disappearance of this band is probably associated with the modification of hydrogen bonds network or the crystal structure due to higher contents of amino groups.[31,33]

According to the results above, the deacetylated chitins in the form of sheets with a DA lower than 0.76 should exhibit a different crystalline structure than the starting α-chitin. Possibly, this new crystalline structure of deacetylated chitins is related to their DA and therefore the formation of different hydrogen bonded network. Thus, the elimination of acetyl groups not only strongly decreases the amount of hydrogen

dx.doi.org/10.1021/jp210469x | J. Phys. Chem. B 2012, 116, 4584−4592

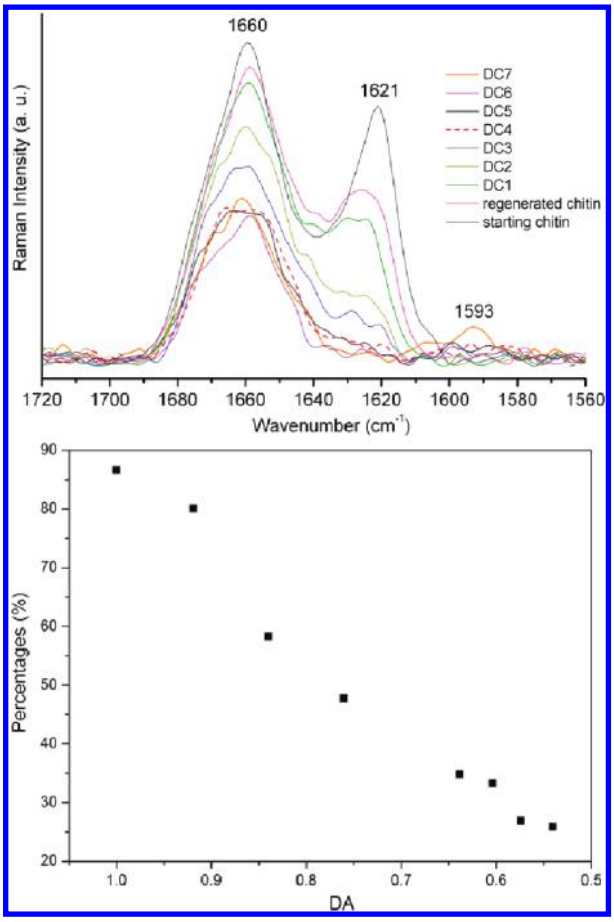

Figure 10. Top: FT Raman spectra (1720−1560 cm^{-1}) of starting, regenerated chitin and deacetylated chitins (DC1−7) at RT. Bottom: The percentages of the areas under the bands at 1688−1604 cm^{-1} within the FT Raman spectrum of regenerated or deacetylated chitins in comparison to starting chitin.

bonds linked to C═O groups in chitin crystals, but also modifies its hydrogen bonded network. As the summary, the variation of DA not only leads to distinct morphologies of chitins, but also changes the hydrogen bonded network forming diverse crystalline structures of chitins.

CONCLUSION

Crab shell α-chitin demonstrated microfibrils with a width of less than 1 μm after the ball-milling in the presence of water. After the homogeneous alkaline deacetylation in the 30% aqueous NaOH solution at 60 °C, various α-chitins with distinct DA were yielded. The microfibrils were destroyed and aggregates or sheets with smooth surfaces were obtained. The DA of modified α-chitins, determined via solid-state CP/MAS ^{13}C NMR spectroscopy, decreased with longer deacetylation durations from 1 to 0.54. The deacetylated chitins with a DA lower than 0.76 exhibited a different crystal structure than that of starting α-chitin based on WAXD measurements. It is possibly due to the formation of a new hydrogen bonded network ascribed to the presence of more amino groups. The amount of hydrogen bonds linked to C═O groups decreased strongly with lower DA, according to the FT Raman signals attributed to the amide groups. Furthermore, FT Raman spectroscopy showed the feasibility of determining the DA of α-chitins with high correlation coefficients greater than 0.99 in relative to those determined by solid-state ^{13}C NMR.

AUTHOR INFORMATION

Corresponding Author

*Tel.: +49 35203 3831239. E-mail: kzhang@forst.tu-dresden.de.

Present Address

⊥110 Agricultural Engineering Building, the Pennsylvania State University, State College, PA, 16802

Notes

The authors declare no competing financial interest.

ACKNOWLEDGMENTS

The financial support by German Research Foundation (Grants: FI755/4-1 and FI755/4-2, GR1290/7-1 and GR1290/7-2) is gratefully acknowledged.

REFERENCES

(1) Muzzarelli, R. A. A.; Muzzarelli, C. *Adv. Polym. Sci.* **2005**, *186*, 151−209.
(2) Rudall, K. M.; Kenching, W. *Biol. Rev. Cambridge Philos. Soc.* **1973**, *48*, 597−633.
(3) Vårum, K. M.; Anthonsen, M. W.; Grasdalen, H.; Smidrød, O. *Carbohydr. Res.* **1991**, *211*, 17−23.
(4) Park, P. J.; Je, J. Y.; Kim, S. K. *Carbohydr. Polym.* **2004**, *55*, 17−22.
(5) Cho, Y.; Jang, J.; Park, C. R.; Ko, S. *Biomacromolecules* **2000**, *1*, 609−614.
(6) Liu, X. F.; Guan, Y. L.; Yang, D.; Li, Z.; Yao, K. D. *J. Appl. Polym. Sci.* **2001**, *79*, 1324−1335.
(7) Tolaimate, A.; Desbrieres, J.; Rhazi, M.; Alagui, A. *Polymer* **2003**, *44*, 7939−7952.
(8) Brugnerotto, J.; Lizardi, J.; Goycoolea, F. M.; Argüelles-Monal, W.; Desbrières, J.; Rinaudo, M. *Polymer* **2001**, *42*, 3569−3580.
(9) Kasaai, M. R. *J. Agric. Food Chem.* **2009**, *57*, 1667−1676.
(10) Prochazkova, S.; Vårum, K. M.; Østgaard, K. *Carbohyd. Polym.* **1999**, *38*, 115−122.
(11) Kumirska, J.; Czerwicka, M.; Kaczyński, Z.; Bychowska, A.; Brzozowski, K.; Thöming, J.; Stepnowski, P. *Mar. Drugs* **2010**, *8*, 1567−1636.
(12) Zhang, Y.; Xue, C.; Xue, Y.; Gao, R.; Zhang, X. *Carbohydr. Res.* **2005**, *340*, 1914−1917.
(13) Heux, L.; Brugnerotto, J.; Desbrières, J.; Versali, M. F.; Rinaudo, M. *Biomacromolecules* **2000**, *1*, 746−751.
(14) Kasaai, M. R. *Carbohydr. Polym.* **2010**, *79*, 801−810.
(15) Colthup, N. B.; Daly, L. H.; Wiberley, S. E. *Introduction to IR and Raman Spectroscopy*, 3rd ed.; Academic Press: London, 1990.
(16) Li, J. F.; Huang, Y. F.; Ding, Y.; Yang, Z. L.; Li, S. B.; Zhou, X. S.; Fan, F. R.; Zhang, W.; Zhou, Z. Y.; Wu, D. Y.; et al. *Nature* **2010**, *464*, 392−395.
(17) Zhang, K.; Helm, J.; Peschel, D.; Gruner, M.; Groth, T.; Fischer, S. *Polymer* **2010**, *51*, 4698−4705.
(18) Muzzarelli, R. A. A. *Chitin*; Pergamon Press: London, 1977.
(19) Carlstrom, D. *J. Biophys. Biochem. Cytol.* **1957**, *3* (5), 669−683.
(20) Minke, R.; Blackwell, J. *Mol. Biol.* **1978**, *120*, 167−181.
(21) Wu, Y.; Sasaki, T.; Irie, S.; Sakurai, K. *Polymer* **2008**, *49*, 2321−2327.
(22) Liu, Y.; Liu, Z.; Pan, W.; Wu, Q. *Carbohydr. Polym.* **2008**, *72*, 235−239.
(23) Noishiki, Y.; Takami, H.; Nishiyama, Y.; Wada, M.; Okada, S.; Kuga, S. *Biomacromolecules* **2003**, *4*, 896−899.
(24) Lamarque, G.; Viton, C.; Domard, A. *Biomacromolecules* **2004**, *5*, 992−1001.
(25) Lamarque, G.; Cretenet, M.; Viton, C.; Domard, A. *Biomacromolecules* **2005**, *6*, 1380−1388.

(26) Methacanon, P.; Prasitsilp, M.; Pothsree, T.; Pattaraarchchai, J. *Carbohydr. Polym.* **2003**, *52*, 119−123.
(27) Ottøy, M. H.; Vårum, K. M.; Smidsrød, O. *Carbohydr. Polym.* **1996**, *29*, 17−23.
(28) Tanner, S. F.; Chanzy, H.; Vincendon, M.; Roux, J. C.; Gaill, F. *Macromolecules* **1990**, *23*, 3576−3583.
(29) Rinaudo, M. *Prog. Polym. Sci.* **2006**, *31*, 603−632.
(30) Chen, P.; Lin, A. Y.; McKittrick, J.; Meyers, M. A. *Acta Biomater.* **2008**, *4*, 587−596.
(31) Okuyama, K.; Noguchi, K.; Miyazawa, T.; Yui, T.; Ogawa, K. *Macromolecules* **1997**, *30*, 5849−5855.
(32) Okuyama, K.; Noguchi, K.; Kanenari, M.; Egawa, T.; Osawa, K. *Carbohydr. Polym.* **2000**, *41*, 237−247.
(33) Sikorski, R.; Hori, R.; Wada, M. *Biomacromolecules* **2009**, *10*, 1100−1105.
(34) Sannan, T.; Kurita, K.; Iwakura, Y. *Makromol. Chem.* **1975**, *176*, 1191−1195.
(35) Sannan, T.; Kurita, K.; Iwakura, Y. *Makromol. Chem.* **1976**, *177*, 3589−3600.
(36) Kurita, K.; Sannan, T.; Iwakura, Y. *Makromol. Chem.* **1977**, *178*, 3197−3202.
(37) Focher, B.; Naggi, A.; Torri, G.; Cosani, A.; Terbojevich, M. *Carbohydr. Polym.* **1992**, *17*, 97−102.
(38) Socrates, G. *Infrared and Raman Characteristic Group Frequencies: Tables and Charts*, 3rd ed.; Wiley: England, 2001.
(39) Pearson, F. G.; Marchessault, R. H.; Liang, C. Y. *J. Polym. Sci.* **1960**, *43*, 101−116.
(40) Schenzel, K.; Fischer, S. *Cellulose* **2001**, *8*, 49−57.